Biointerface Research in Applied Chemistry
Open-Access Journal (ISSN: 2069-5837)

Article
Volume 13, Issue 6, 2023, 583
https://doi.org/10.33263/BRIAC136.583

Antifungal Activity of Biosynthesized Silver Nanoparticles Mediated by Neem Leaf Extract against *Aspergillus* sp.

Wan Nur Atiqah Wan Shamsudin [1], Che Ku Mohammad Faizal Che Ku Yahya [2], Siti Hajar Noor Shaarani [3,*]

[1] Faculty of Chemical and Process Engineering Technology, Universiti Malaysia Pahang, 26300 Gambang, Pahang, Malaysia; watiqah19@gmail.com (W.N.A.W.S); mfaizal@ump.edu.my (C.K.M.F.C.K.Y); hajarnoor@ump.edu.my (S.H.N.S);
* Correspondence: hajarnoor@ump.edu.my (S.H.N.S);

Scopus Author ID 56335600100
Received: 1.12.2022; Accepted: 11.01.2023; Published: 2.04.2023

Abstract: Silver nanoparticles (AgNPs) have attracted considerable attraction as excellent antifungal agents against various pathogens. In the present study, AgNPs were biosynthesized using neem leaf aqueous extract, and their antifungal properties were evaluated against *Aspergillus* sp. The formation of newly synthesized AgNPs was confirmed through visual observation by a change in the color of the solution, followed by an analysis of their surface plasmon resonance via UV-vis spectrophotometer. Further characterization of its crystalline nature and morphology structure was assessed by X-Ray Diffraction (XRD) and Field-emission Scanning Electron Microscope (FESEM), respectively. The result revealed that the synthesized AgNPs showed UV-vis spectra peak around 421 nm, are crystalline in nature, and have a spherical morphology with an average size of 20.13 ± 3.3 nm in diameter. Furthermore, these AgNPs exhibit excellent antifungal activity against the waterborne pathogen *Aspergillus* sp. on agar well diffusion assay with a maximum 26.54 ± 1.23 mm zone of inhibition. FESEM image revealed hyphal damage and deformation of fungus when treated with AgNPs, causing retardation of fungus growth for further reproduction. The results suggested that this biosynthesis AgNPs from neem leaf extract has great potential as an alternative antifungal agent for use in water treatment.

Keywords: antifungal activity; biosynthesis; silver nanoparticles; neem leaves; *Aspergillus* sp.

1. Introduction

Water is essential for almost every living organism to sustain its living mechanism. Therefore, every effort has to be made to achieve safe drinking water for consumer health security. The presence of microbial contaminants, such as pathogenic fungi, in the water distribution systems, can deteriorate the quality of the delivered water. Some of the fungus species are capable of producing secondary metabolites or mycotoxins that are toxic and thus have an adverse impact on human health [1–3]. Waterborne filamentous fungi from the genera *Aspergillus* is a potentially pathogenic fungus commonly detected and isolated from treated and untreated drinking water systems [4,5]. Studies found that fungal *Aspergillus* is prone to cause allergenic responses risking immuno-competent individuals [6]. Several species from the *Aspergillus* genera have been identified to generate mycotoxins that are hazardous to human health [7,8]. The most widespread strategies used to control fungi in the water treatment system mainly were chlorine and chloramine, which are associated with the formation of disinfection

by-products (DBP) [9,10]. In addition, the isolation of pathogen fungi in treated water proves that the current strategies are not adequate to remove this contaminant. Therefore, an alternative practice that has promising features in efficiency and is more environmentally friendly is urgently needed to inhibit and eradicate fungus pathogens from water.

The application of nanotechnology in water treatment has drawn wide attention due to its notable ability to remove contaminants and thus can potentially be an alternative to replace conventional water treatment systems [11–13]. Nanoscale features with particles size ranging from 1 nm to 100 nm make nanoparticles of great interest in diverse applications, including as antimicrobial agents [14]. Among all metal nanoparticles, silver nanoparticles (AgNPs) are well-known for their distinctive, unique properties, specifically as an antimicrobial agent against a broad spectrum of pathogens [14,15]. The synthesis of AgNPs has been employed using physical, chemical, and biological methods. The downside of utilizing physical and chemical methods is that it is rather time-consuming, costly, and possibly produce by-products that are potentially toxic [16]. Consequently, using biological sources, including bacteria, algae, fungi, and plant-based material, as a green approach to synthesizing AgNPs possesses great advantages as they are simple, less time-consuming, and more environmentally friendly.

Various plant extract has been utilized for the green synthesis of AgNPs owing to the phytochemical constituents found in plant materials. These constituents, like phenols, flavonoids, and terpenoids, are known to function as reducing and stabilizing agents in nanoparticle synthesis from its precursor salt [17]. Several studies reported the green synthesis of AgNPs from various medicinal plant extracts exhibits excellent antifungal activity against some important pathogens. The medicinal plant includes *Medicago sativa* [18], *Portulaca oleracea* [19], *Allium saralicum* [20], *Rubia cordifolia* [21], and *Phoenix Dactylifera* [15]. Another competent medicinal plant that is widely exploited for its benefits in traditional medical treatment and the agricultural industry is *Azadirachta indica* or neem. The neem tree was cultivated extensively in Malaysia for its medicinal values, such as antibacterial, antifungal, antioxidant, anti-inflammatory, and anticancer [22,23]. Abundant phytochemical constituent in a different part of the neem tree has a great perspective in the field of pest management, medicine, and environmental protection.

Incorporation of benefit from neem with silver to form AgNPs, allowing enhanced antifungal activities against targeted pathogens. Therefore, this study aimed to synthesize AgNPs mediated by neem leaf extract, evaluate its antifungal efficiency against isolated waterborne pathogen *Aspergillus* sp., and assess the morphology of treated fungi after AgNPs exposure by employing FESEM analysis.

2. Materials and Methods

2.1. Materials.

Neem leaves were collected around Kuantan, Pahang region. The *Aspergillus* sp. fungus strain was retrieved from the Microbiology lab at the Faculty of Chemical and Process Engineering Technology, Universiti Malaysia Pahang. Silver nitrate ($AgNO_3$) was purchased from Sigma Aldrich, USA, with ≥ 99.99% purity.

2.2. Preparation of neem leaf extract.

Dried neem leaves were grounded into a fine powder and passed through a sieve to obtain a uniform powder size. 10 g of dried neem leaf powder was extracted with 100 mL of distilled water. The extraction was done on a magnetic stirrer with continuous agitation at a constant rate for 24 h at room temperature. The solution was then filtered through a Whatman filter No.1, and the clear solution was centrifuged at 4000 rpm for 15 mins. The filtrate was quickly frozen at -80°C for 24 h and lyophilized by a freeze dryer for 48 h to produce a powdered form of neem leaf extract. A stock solution that is being used throughout the study was prepared at a concentration of 1 mg/mL in distilled water.

2.3. Phytochemical profiling in neem leaves extract.

Phytochemical profiling of neem leaves aqueous extract was carried out using Liquid Chromatography Coupled to Quadrupole Time-of-Flight Mass Spectrometry (LC-QTOF MS, Waters, Milford, MA, USA) using the method described by [24] with a modification. The separation was done using a C18 column (ACQUITY UPLC BEH C18 (2.1 × 50 mm, 1.7 µm); Waters, Milford, MA, USA). Solvent Name A: Water + 0.1% Formic Acid and Solvent Name B: Acetonitrile + 0.1% Formic Acid was used as the mobile phase with a flow rate of 0.5 mL/min, and the injection volume was 5 µL for each sample. The gradient elution program was; 0-0.5 min, 1% solvent B; 0.5-16 min, 35% solvent B; 16-18 min, 100% solvent B; 18-20 min, 1% solvent B.

2.4. Synthesis of AgNPs.

Synthesis of AgNPs by neem leaves extract was prepared following a method described by Chinnasamy *et al*. [25] with modification. Briefly, 90 mL of 1 mM $AgNO_3$ solution was added to 10 mL of neem leaves extract stock solution (9:1 ratio). The resultant mixture was then incubated in a dark incubator chamber at a constant speed of 150 rpm and maintained at 60°C for 24 h. Afterward, the suspension of synthesized AgNPs was separated by centrifugation method at 14,000 rpm for 15 mins, and the nanoparticles were air dried for further use and characterization.

2.5. Characterization of AgNPs.

The formation of nanoparticles was determined by the change in visual color of the solution from light yellow to reddish brown, and the UV spectrum of the reaction solution was measured and monitored in the wavelength range from 300 nm to 800 nm using a UV-Visible spectrophotometer (UV-Vis, Shimadzu UV-2450). The possible functional group involved in the synthesis of AgNPs was identified using Fourier Transform Infrared Spectroscopy (FTIR) analysis (Thermo Scientific Nicolet iS50). The spectra were recorded in the range of 400 to 4000 cm^{-1}. The crystalline structure of synthesized AgNPs was assessed with X-ray diffraction (XRD) scanning (D8 Advance, Bruker, Germany) within the range of 30°–80° at 2θ. Morphological characterization, including size, shape, and distribution pattern of synthesized nanoparticles, was analyzed using field emission scanning electron microscopy (FESEM; JEOL-JSM-7800F) and measured using ImageJ software.

2.6. Antifungal activity of AgNPs.

The antifungal activity of synthesized AgNPs from neem leaf extract was assessed by using an agar well diffusion assay against a waterborne pathogen, *Aspergillus* sp. A sterile

cotton swab loaded with fungal suspension with a number of approximately 1.5×10^8 CFU/mL was spread evenly on Potato Dextrose Agar (PDA) plates. Wells were made on the agar plates using a sterile borer, and 100 µl of varied concentrations of AgNPs (10-100 µg/mL) were introduced to each well to compare their antifungal performance. Well, without treatment was used as the negative control. The plates were incubated at 28°C for 24 h to determine the diameter (mm) of the zone of inhibition (ZOI) around each well.

2.7. Morphological visualization on Aspergillus sp. Hyphae under AgNPs exposure.

Structural changes in *Aspergillus* sp. Hyphae after exposure to synthesized AgNPs were observed by using field emission scanning electron microscopy (FE-SEM; JSM-7800F) imaging. *Aspergillus* sp. Conidial suspension (1.5×10^8 CFU/mL) was added to 10 mL of sterile saline water treated with AgNPs. The cultures were agitated by constant shaking in an incubating shaker for 24 h at 28 ± 2°C [26]. After 4 h treatment, the treated fungal cells were then harvested by centrifugation method at 3000 rpm for 30 mins. The pellets were rinsed three times with phosphate-buffered saline (PBS) before being fixed with 2.5% glutaraldehyde. The pellets were re-rinsed with PBS, and the dehydration process was carried out with a series of increasing ethanol concentrations. Lastly, the samples were air-dried, gold coated, and examined.

3. Results and Discussion

3.1. Phytochemical profiling in neem leaf extract.

LC QTOF MS analysis revealed that this study's neem leaf aqueous extract is rich in flavonoid and terpenoid compounds. Table 1 presents six major phytochemical constituents along with their possible bioactivities, which may be employed as the reducing and stabilizing agents during the synthesis of AgNPs. These compounds strongly influence the reduction process of silver ions to silver nanoparticles and stabilize silver ions to prevent aggregations of nanoparticles [27]. Some phytochemicals are known for their antihyperglycemic, antioxidative, and anticancer activities. In addition, the antioxidative properties of the plant extract are reported for their attribution in reducing metal ions to nanoparticles [28].

Table 1. Major phytochemical constituents identified in the aqueous extract of neem leaf extract.

Compound	Molecular Formula	Chemical Structure	RT (min)	Biological Activity
8-Debenzoylpaeoniflorin	$C_{16}H_{24}O_{10}$	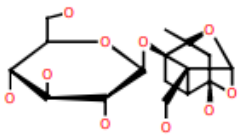	1.21	Antihyperglycemic [29]
Icariside B4	$C_{19}H_{32}O_8$	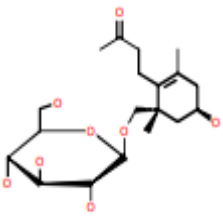	7.55	Not reported

Compound	Molecular Formula	Chemical Structure	RT (min)	Biological Activity
Picrasinoside A	$C_{27}H_{38}O_{11}$	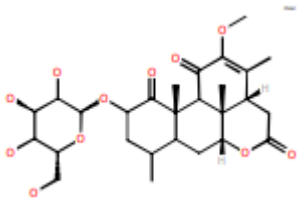	10.10	Not reported
4,8,12-Trimethyl-tridecanoic acid	$C_{16}H_{32}O_2$	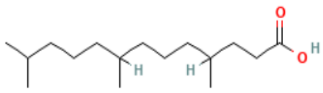	16.52	Not reported
11-O-p-Coumarylnepeticin	$C_{39}H_{56}O_4$	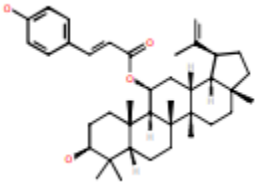	17.26	Antioxidative [30]
Ganoderic acid S	$C_{30}H_{44}O_3$	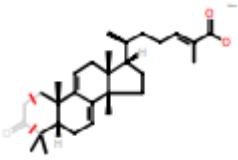	18.34	Anticancer [31]

3.2. Visual observation of AgNPs synthesis.

The primary indication for the formation of AgNPs is by visual observation of the change in color of the colloidal solution from light yellow to reddish brown (Figure 1). The color change indicates the reduction process from Ag^+ to Ag^0 with the presence of a reducing agent [32]. A previous investigation by Pandian *et al*. [34] also had a similar color formation suggesting a complete reaction of neem leaf extracts with precursor $AgNO_3$. It has been reported that phytochemical constituents present in neem leaf extract are mainly responsible for reducing and stabilizing agents for the production and synthesis of AgNPs [14,33].

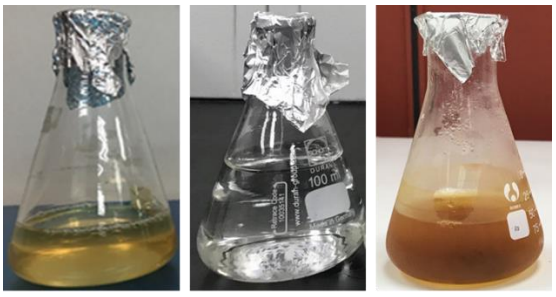

(a) **(b)** **(c)**

Figure 1. Green synthesis of AgNPs by neem leaves extracts **(a)** Neem leaf extract; **(b)** 1mM $AgNO_3$ solution; **(c)** colloidal of AgNPs.

3.3. UV-vis spectroscopy analysis.

Uv-visible spectroscopy analysis provides information on the surface plasmon resonance (SPR) band that is formed due to the interaction between electrons of silver nanoparticles and light waves [35]. Figure 2 shows the UV-visible spectral band of synthesized AgNPs compared with neem leaf extract and $AgNO_3$ as a control. A peak on the SPR band was detected around 421 nm on AgNPs, while 1 mM of $AgNO_3$ and neem leaves extract shows no characteristic peak, further validating the formation of AgNPs. AgNPs synthesized by neem leaf extract, as reported in the previous study, correspond to the absorption peak on the SPR band around 420-470 nm[36–38].

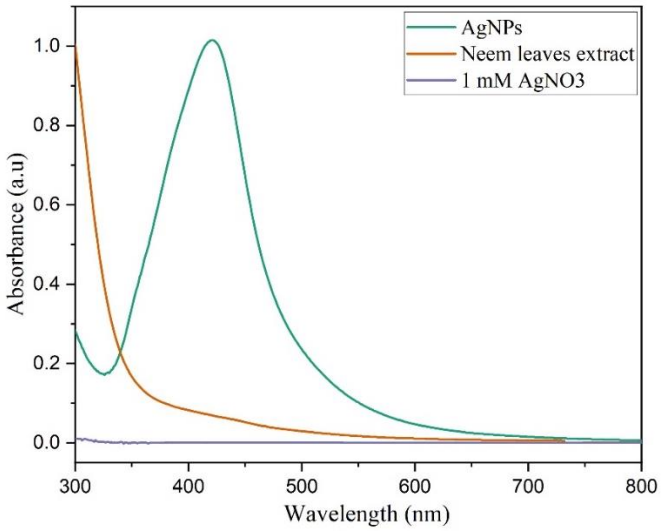

Figure 2. UV–vis absorption spectra of synthesized AgNPs compared to precursor salt $AgNO_3$ and neem leaves extract.

3.4. FTIR (Fourier Transform Infrared) analysis.

As shown in Figure 3, the FTIR spectra of neem leaf extract and AgNPs revealed several distinct peaks corresponding to functional groups involved in the reduction of AgNPs. The peaks in neem leaf extract at a wavenumber of 3389.40 cm^{-1}, 1643.99 cm^{-1}, and 637.96 cm^{-1} are corresponded to hydroxyl (O-H) stretching of alcohol and phenol [39], stretching of alkene (C=C) group [26] and alkyl halides (C-Br) group (out of plane vibration) respectively. The vibrational bands were shifted to 3389.49 cm^{-1}, 1644.08 cm^{-1}, and 637.98 cm^{-1} in synthesized AgNPs, indicating the interaction of phenol, alkene, and alkyl halides of neem leaf extract in the reduction and synthesis of AgNPs.

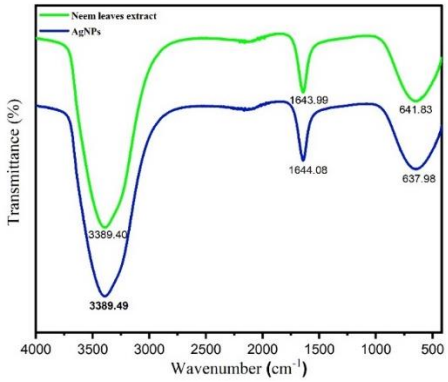

Figure 3. FTIR spectrum of neem leaf extract and AgNPs.

3.5. X-ray diffraction (XRD).

The powdered synthesized AgNP was characterized for its crystalline structure at different phases using XRD analysis. All peaks correspond to AgNPs composed of pure silver compared to the standard silver diffraction card of International Center for Diffraction Data (ICDD), silver file No. 04-0783. As shown in Figure 4, several diffraction peaks were observed at 2θ values of 38.09°, 44.36°, 64.17° and 77.54° corresponding to the planes of (1 1 1), (2 0 0), (2 2 0), and (3 1 1) respectively. These peaks reflect the face-centered cubic (fcc) structure of metallic silver [21]. The average crystallite size of AgNPs was calculated by using the Debye-Scherrer formula [40].

$$D = K\lambda/\beta cos\theta$$

where D is the particle size, K is the constant having value of 0.9, λ is the wavelength of Cu-kα (1.54056 Å) X-ray, β represents full width at half maximum (FWHM) angle, and θ is the peak corresponding to diffraction angle. Based on the equation, the estimated average crystallite size of AgNPs was found to be 16.44 nm.

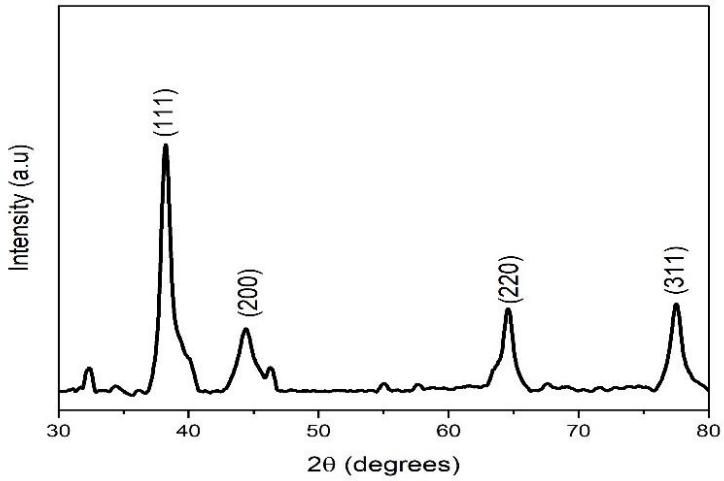

Figure 4. XRD spectrum of synthesized AgNPs.

3.6 Field Emission Scanning Electron Microscope analysis

FESEM analysis provides insight into the morphology and size of AgNPs produced.

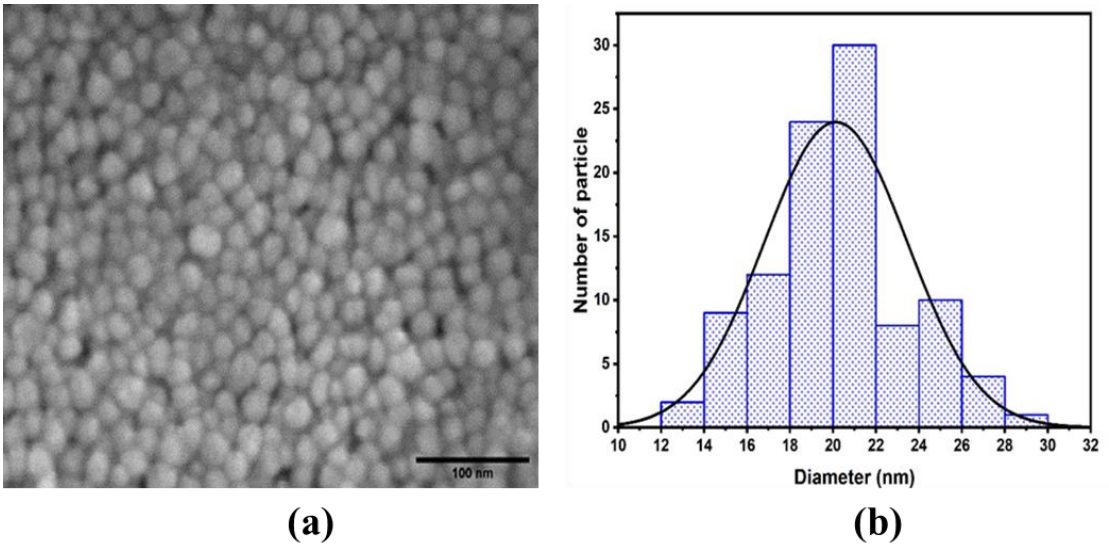

Figure 5. FESEM image of **(a)** morphology of synthesized AgNPs at 100nm magnification level; **(b)** Particle size distribution of synthesized AgNPs.

As illustrated in Figure 5 (a), the result revealed that AgNPs synthesized by neem leaf extract were almost spherical, had smooth surfaces, were uniformly distributed, and were less agglomerate. AgNPs produced exhibit particles in size range from 12 – 28 nm with an average size of 20.13 ± 3.3 nm (Figure 4). A similar configuration from the previous study conducted by Asimuddin *et al*. [41], where AgNPs synthesized by neem leaf extract produced nanoparticles in spherical shape within the size range from 20 -50 nm.

3.7 Antifungal Activity of AgNPs

Agar well diffusion assay was used to evaluate antifungal activity on different concentrations of AgNPs against *Aspergillus* sp. based on ZOI, and the result is summarized in Table 2. Evaluation for antifungal test on neem leaves extract was done to elucidate its effect on antifungal activity of synthesized AgNPs against *Aspergillus* sp. Based on the result, neem leaf extract does not possess antifungal activity resulting in no ZOI, suggesting that the antifungal activity of synthesized AgNPs did not depend on neem leaf extract. The lack of antifungal activity in neem leaf extract may be due to the low concentration and nature of the solvent for extraction used throughout the study. AgNPs synthesized by neem leaf extract exert excellent antifungal activity forming a clear inhibition zone in all concentrations regardless of a lower concentration, as shown in Figure 6. The maximum and minimum inhibition zone formed by AgNPs against *Aspergillu*s sp. was 26.54 ± 1.23 mm and 17.76 ± 0.54 mm, respectively. A similar antifungal effect of silver nanoparticles mediated by neem leaf extract was observed against phytopathogen isolated from an infected brinjal plant studied by Haroon *et al*. [42]. AgNPs produced showed fungicidal activity against the fungus *Penicillium* sp., *Fusarium* sp., and *Aspergillus* sp. with 92%, 89%, and 69% radial growth reduction after 6 days of treatment, respectively. These results depict the effectiveness of green synthesized AgNPs by neem leaf extract against the fungus *Aspergillus* sp. Several researchers demonstrated that the morphology of the nanoparticles significantly influences their antimicrobial activity. The smaller size of particles provides higher surface volume, which creates an extensive contact area for the interaction of silver ions with targeted pathogen [14,43]. Accumulation of silver ions can disrupt the electron transport system, leading to cell disintegration, thus suppressing the growth of fungus [44].

Table 2. Comparison of antifungal activity against *Aspergillus* sp. based on the diameter of zone of inhibition (ZOI).

Fungus	Zone of Inhibition (mm)						
	Neem leaves extract	AgNPs (µg/mL)					
		10	20	40	60	80	100
Aspergillus sp.	0	17.76 ± 0.54 mm	19.74 ± 0.47 mm	21.43 ± 0.52 mm	22.28 ± 0.80 mm	22.49 ± 1.08 mm	26.54 ± 1.23 mm

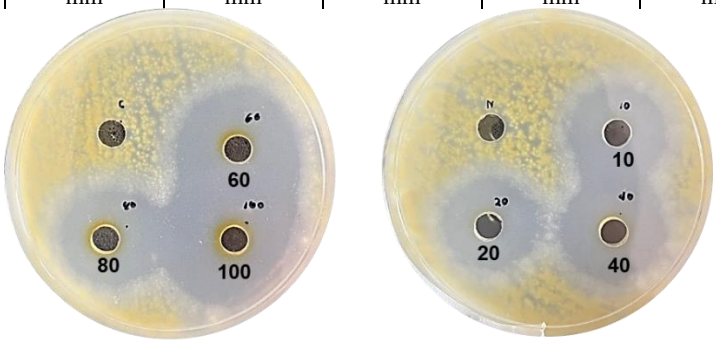

Figure 6. Antifungal test on *Aspergillus* sp, using agar well diffusion assay.

3.8 Morphology of Aspergillus sp. hyphal under AgNPs exposure.

Hyphae is a tubular projection of filamentous fungi that are involved in nutrient absorption uptake to maintain and regulate fungal cells' normal functioning. Alteration of fungal hyphal morphology will disrupt vital cellular functioning, causing dysfunctionalities of cells, thus potentially retard fungus growth for further reproduction [45]. FESEM analysis illustrates direct visualization of the morphological changes in the hyphal structure of fungus treated with synthesized AgNPs. As shown in Figure 7, microscopic observation displays smooth, linear, and still intact fungus hyphae in the absence of AgNPs (control). In contrast, fungus treated with AgNPs showed the appearance of slight hyphal shrinkage, severe malformation, and exceptional cell damage compared with control hyphal cells. Similar effects on structural changes of fungal hyphae upon exposure to biosynthesized AgNPs were observed on the filamentous fungus *Aspergillus niger* where the cell walls of fungal hyphae showed dried and exceptional structural shrinkage [46]. Dakal *et al*. [45] proposed that the observed damage of fungal cells was exerted by releasing silver ions from AgNPs. Silver ions adhere to the cell wall or cell membrane and perforate into the cells, resulting in serious and varied alterations in cell physiology, causing changes to the intracellular structure of the fungus. Consequently, alterations in the physiological state of cells induce cell death.

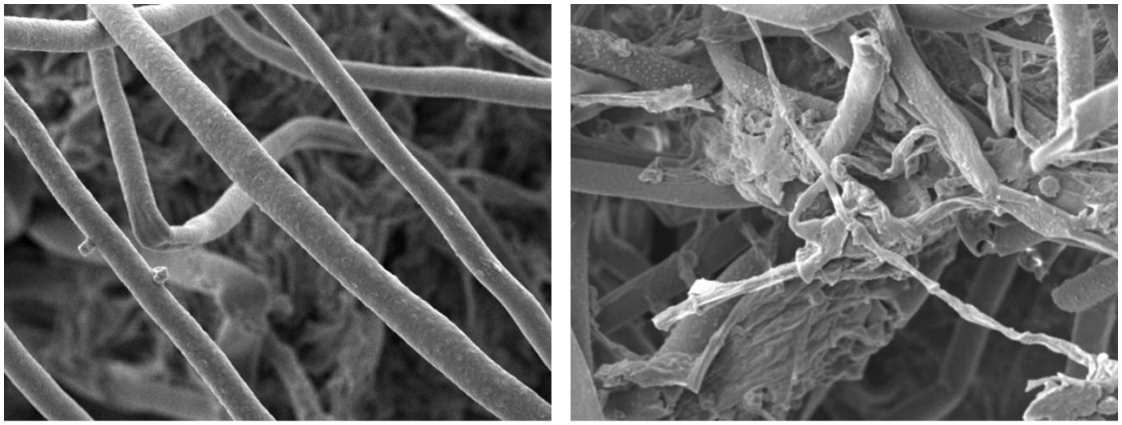

Figure 7. FESEM image showing hyphae structure of *Aspergillus* sp. **(a)** control (without AgNPs), **(b)** cells treated with AgNPs.

4. Conclusion

Silver nanoparticles synthesized by neem leaf extract are simple, cost-effective, and environmentally friendly. The finding suggests that synthesized silver nanoparticles can be used as an antifungal agent in water treatment. Major phytochemical constituent in neem leaves aqueous extracts that served as reducing and capping agents for the synthesis of AgNPs are found to be 8- Debenzoylpaeoniflorin, Icariside B4, Picrasinoside A 4,8,12-Trimethyl-tridecanoic acid, 11-O-p-Coumarylnepeticin, and Ganoderic acid S. AgNPs produced have particles with an average size of 20.13 ± 3.3 nm and exhibit excellent antifungal activities against *Aspergillus* spp. Further studies for optimization and feasibility study of AgNPs as disinfectants in water treatment need to be conducted for industrial applications.

Funding

This research was funded by the Ministry of Higher Education under Fundamental Research Grant Scheme FRGS/1/2019/TK10/UMP/02/3 (RDU 1901118) and Universiti Malaysia Pahang Research Grant (RDU200721).

Acknowledgments

The authors would like to express sincere gratitude to the Faculty of Chemical Engineering and Technology process for providing us with an instrumentation facility used in the characterization process.

Conflicts of Interest

The authors declare no conflict of interest.

References

1. Arroyo, M.G.; Ferreira, A.M.; Frota, O.P.; Brizzotti-Mazuchi, N.S.; Peresi, J.T.M.R.; Rigotti, M.A.; MacEdo, C.E.; Sousa, A.F.L. De; Andrade, D. De; Almeida, M.T.G. De. Broad Diversity of Fungi in Hospital Water. *Scientific World Journal* **2020**, *2020*, https://doi.org/10.1155/2020/9358542.
2. Al-Gabr, H.M.; Zheng, T.; Yu, X. Fungi Contamination of Drinking Water. *Reviews of Environmental Contamination and Toxicology* **2014**, *228*, 121–139, https://doi.org/10.1007/978-3-319-01619-1_6.
3. Cao, R.; Wan, Q.; Tan, L.; Xu, X.; Wu, G.; Wang, J.; Xu, H.; Huang, T.; Wen, G. Evaluation of the Vital Viability and Their Application in Fungal Spores' Disinfection with Flow Cytometry. *Chemosphere* **2021**, Elsevier Ltd *269*, 128700, https://doi.org/10.1016/j.chemosphere.2020.128700.
4. Mhlongo, T.N.; Ogola, H.J.O.; Selvarajan, R.; Sibanda, T.; Kamika, I.; Tekere, M. Occurrence and Diversity of Waterborne Fungi and Associated Mycotoxins in Treated Drinking Water Distribution System in South Africa: Implications on Water Quality and Public Health. *Environmental Monitoring and Assessment* **2020**, Environmental Monitoring and Assessment *192*, https://doi.org/10.1007/s10661-020-08477-x.
5. Afonso, T.B.; Simões, L.C.; Lima, N. Occurrence of Filamentous Fungi in Drinking Water: Their Role on Fungal-Bacterial Biofilm Formation. *Research in Microbiology* **2021**, *172*, https://doi.org/10.1016/j.resmic.2020.11.002.
6. Bandh, S.A.; Kamili, A.N.; Ganai, B.A.; Lone, B.A. Opportunistic Fungi in Lake Water and Fungal Infections in Associated Human Population in Dal Lake, Kashmir. *Microbial Pathogenesis* **2016**, Elsevier Ltd *93*, 105–110, https://doi.org/10.1016/j.micpath.2016.01.022.
7. Navale, V.; Vamkudoth, K.R.; Ajmera, S.; Dhuri, V. Aspergillus Derived Mycotoxins in Food and the Environment: Prevalence, Detection, and Toxicity. *Toxicology Reports* **2021**, *8*, 1008–1030, https://doi.org/10.1016/j.toxrep.2021.04.013.
8. Ráduly, Z.; Szabó, L.; Madar, A.; Pócsi, I.; Csernoch, L. Toxicological and Medical Aspects of Aspergillus-Derived Mycotoxins Entering the Feed and Food Chain. *Frontiers in Microbiology* **2020**, *10*, 1–23, https://doi.org/10.3389/fmicb.2019.02908.
9. Li, X.F.; Mitch, W.A. Drinking Water Disinfection By-products (DBPs) and Human Health Effects: Multidisciplinary Challenges and Opportunities. *Environmental Science and Technology* **2018**, *52*, 1681–1689, https://doi.org/10.1021/acs.est.7b05440.
10. Hu, Z.T.; Chen, Y.; Fei, Y.F.; Loo, S.L.; Chen, G.; Hu, M.; Song, Y.; Zhao, J.; Zhang, Y.; Wang, J. An Overview of Nanomaterial-Based Novel Disinfection Technologies for Harmful Microorganisms: Mechanism, Synthesis, Devices and Application. *Science of the Total Environment* **2022**, Elsevier B.V. *837*, 155720, https://doi.org/10.1016/j.scitotenv.2022.155720.
11. Bhardwaj, A.K.; Sundaram, S.; Yadav, K.K.; Srivastav, A.L. An Overview of Silver Nanoparticles as Promising Materials for Water Disinfection. *Environmental Technology and Innovation* **2021**, Elsevier B.V. *23*, 101721, https://doi.org/10.1016/j.eti.2021.101721.
12. Nayak, S.; Concepta, L.; Kumar, P.S.; Selvaraj, R. Plant-Mediated Gold and Silver Nanoparticles as Detectors of Heavy Metal Contamination. *Food and Chemical Toxicology* **2022**, Elsevier Ltd *167*, 113271, https://doi.org/10.1016/j.fct.2022.113271.
13. Magalhães-Ghiotto, G.A.V.; Oliveira, A.M. d.; Natal, J.P.S.; Bergamasco, R.; Gomes, R.G. Green Nanoparticles in Water Treatment: A Review of Research Trends, Applications, Environmental Aspects and Large-Scale Production. *Environmental Nanotechnology, Monitoring and Management* **2021**, *16*, 100526, https://doi.org/10.1016/j.enmm.2021.100526.
14. Huq, M.A.; Ashrafudoulla, M.; Rahman, M.M.; Balusamy, S.R.; Akter, S. Green Synthesis and Potential

Antibacterial Applications of Bioactive Silver Nanoparticles: A Review. *Polymers* **2022**, *14*, 1–22, https://doi.org/10.3390/polym14040742.
15. Al Mutairi, J.F.; Al-Otibi, F.; Alhajri, H.M.; Alharbi, R.I.; Alarifi, S.; Alterary, S.S. Antimicrobial Activity of Green Silver Nanoparticles Synthesized by Different Extracts from the Leaves of Saudi Palm Tree (Phoenix Dactylifera L.). *Molecules* **2022**, *27*, 3113, https://doi.org/10.3390/molecules27103113.
16. Arshad, H.; Saleem, M.; Pasha, U.; Sadaf, S. Synthesis of Aloe Vera-Conjugated Silver Nanoparticles for Use against Multidrug-Resistant Microorganisms. *Electronic Journal of Biotechnology* **2022**, Pontificia Universidad Católica de Valparaíso *55*, 55–64, https://doi.org/10.1016/j.ejbt.2021.11.003.
17. Nayak, S.; Sajankila, S.P.; Goveas, L.C.; Rao, V.C.; Mutalik, S.; Shreya, B.A. Two Fold Increase in Synthesis of Gold Nanoparticles Assisted by Proteins and Phenolic Compounds in Pongamia Seed Cake Extract: Response Surface Methodology Approach. *SN Applied Sciences* **2020**, *2*, 1–12, https://doi.org/10.1007/s42452-020-2348-5.
18. Zare-Bidaki, M.; Aramjoo, H.; Mizwari, Z.M.; Mohammadparast-Tabas, P.; Javanshir, R.; Mortazavi-Derazkola, S. Cytotoxicity, Antifungal, Antioxidant, Antibacterial and Photodegradation Potential of Silver Nanoparticles Mediated via Medicago Sativa Extract. *Arabian Journal of Chemistry* **2022**, *15*, 103842, https://doi.org/10.1016/j.arabjc.2022.103842.
19. Al-Otibi, F.; Alfuzan, S.A.; Alharbi, R.I.; Al-Askar, A.A.; AL-Otaibi, R.M.; Al Subaie, H.F.; Moubayed, N.M.S. Comparative Study of Antifungal Activity of Two Preparations of Green Silver Nanoparticles from Portulaca Oleracea Extract. *Saudi Journal of Biological Sciences* **2022**, *29*, 2772–2781, https://doi.org/10.1016/j.sjbs.2021.12.056.
20. Zangeneh, M.M.; Bovandi, S.; Gharehyakheh, S.; Zangeneh, A.; Irani, P. Green Synthesis and Chemical Characterization of Silver Nanoparticles Obtained Using Allium Saralicum Aqueous Extract and Survey of in Vitro Antioxidant, Cytotoxic, Antibacterial and Antifungal Properties. *Applied Organometallic Chemistry* **2019**, *33*, 1–11, https://doi.org/10.1002/aoc.4961.
21. Chandraker, S.K.; Lal, M.; Khanam, F.; Dhruve, P.; Singh, R.P.; Shukla, R. Therapeutic Potential of Biogenic and Optimized Silver Nanoparticles Using Rubia Cordifolia L. Leaf Extract. *Scientific Reports* **2022**, *12*, 1–15, https://doi.org/10.1038/s41598-022-12878-y.
22. Akhtar, M.S.; Swamy, M.K.; Sinniah, U.R. Natural Bio-Active Compounds. *Natural Bio-active Compounds: Production and Applications* **2019**, *1*, 1–608, https://doi.org/10.1007/978-981-13-7154-7.
23. Mohideen, M.; Syamimi, N.; Zainal, I. An Overview of Antibacterial and Antifungal Effects of Azadirachta Indica Crude Extract : *A Narrative Review*. **2022**, *15*, 505–514,. https://dx.doi.org/10.13005/bpj/2391.
24. Tang, J.; Dunshea, F.R.; Suleria, H.A.R. LC-ESI-QTOF/MS Characterization of Phenolic Compounds from Medicinal Plants (Hops and Juniper Berries) and Their Antioxidant Activity. *Foods* **2020**, *9*, 1–25, https://doi.org/10.3390/foods9010007.
25. Chinnasamy, G.; Chandrasekharan, S.; Koh, T.W.; Bhatnagar, S. Synthesis, Characterization, Antibacterial and Wound Healing Efficacy of Silver Nanoparticles From Azadirachta Indica. *Frontiers in Microbiology* **2021**, *12*, 1–14, https://doi.org/10.3389/fmicb.2021.611560.
26. Ali, E.M.; Abdallah, B.M. Effective Inhibition of Invasive Pulmonary Aspergillosis by Silver Nanoparticles Biosynthesized with Artemisia Sieberi Leaf Extract. **2022**,. https://doi.org/10.3390/nano12010051.
27. Mustapha, T.; Misni, N.; Ithnin, N.R.; Daskum, A.M.; Unyah, N.Z. A Review on Plants and Microorganisms Mediated Synthesis of Silver Nanoparticles, Role of Plants Metabolites and Applications. *International Journal of Environmental Research and Public Health* **2022**, *19*, https://doi.org/10.3390/ijerph19020674.
28. Pradeep, M.; Kruszka, D.; Kachlicki, P.; Mondal, D.; Franklin, G. Uncovering the Phytochemical Basis and the Mechanism of Plant Extract-Mediated Eco-Friendly Synthesis of Silver Nanoparticles Using Ultra-Performance Liquid Chromatography Coupled with a Photodiode Array and High-Resolution Mass Spectrometry. *ACS Sustainable Chemistry and Engineering* **2022**, *10*, 562–571, https://doi.org/10.1021/acssuschemeng.1c06960.
29. Hsu, F.L.; Lai, C.W.; Cheng, J.T. Antihyperglycemic Effects of Paeoniflorin and 8-Debenzoylpaeoniflorin, Glucosides from the Root of Paeonia Lactiflora. *Planta Medica* **1997**, *63*, 323–325, https://doi.org/10.1055/s-2006-957692.
30. Harun, A.; Aziz, N.A.; Azenan, N.S.M.; Kamarazzaman, N.F.M.; Mat So'Ad, S.Z. Antimicrobial Efficacy, Antioxidant Profile and Nine Alternative Active Constituents from Petroleum Ether and Ethyl Acetate Extract of Entada Spiralis. *Malaysian Journal of Analytical Sciences* **2020**, *24*, 707–718,. https://mjas.analis.com.my/mjas/v24_n5/pdf/Aiza_24_5_8.pdf.
31. Liu, R.M.; Zhong, J.J. Ganoderic Acid Mf and S Induce Mitochondria Mediated Apoptosis in Human Cervical Carcinoma HeLa Cells. *Phytomedicine* **2011**,. *18*, 349–355, https://doi.org/10.1016/j.phymed.2010.08.019.
32. Ahmed, R.H.; Mustafa, D.E. Green Synthesis of Silver Nanoparticles Mediated by Traditionally Used Medicinal Plants in Sudan. *International Nano Letters* **2020**, *10*, 1–14, https://doi.org/10.1007/s40089-019-00291-9.
33. Hano, C.; Abbasi, B.H. Plant-Based Green Synthesis of Nanoparticles: Production, Characterization and Applications. *Biomolecules* **2022**, *12*, 1–9, https://doi.org/10.3390/biom12010031.
34. Pandian, H.; Senthilkumar; Ratnam M, V.; M, N.; S, S. Azadirachta Indica Leaf Extract Mediated Silver

Nanoparticles Impregnated Nano Composite Film (AgNP/MCC/Starch/Whey Protein) for Food Packaging Applications. *Environmental Research* **2023**, *216*, 114641, https://doi.org/10.1016/j.envres.2022.114641.
35. Usmani, A.; Mishra, A.; Jafri, A.; Arshad, M.; Siddiqui, M.A. Green Synthesis of Silver Nanocomposites of Nigella Sativa Seeds Extract for Hepatocellular Carcinoma. *Current Nanomaterials* **2019**, *4*, 191–200, https://doi.org/10.2174/2468187309666190906130115.
36. Mishra, R.; Gwalani, K.; Nashikkar, N.; Bundale, S. Antibacterial and Anti-Quorum Sensing Studies of Extracellularly Synthesized Silver Nanoparticles from Azadirachta Indica (Neem) Leaf Extract. *Biosciences Biotechnology Research Asia* **2022**, *19*, 1065–1078,. http://dx.doi.org/10.13005/bbra/3056.
37. Indica, M.; Indica, A.; Extract, L.; Barnabas, H.L.; Markus, A.; Gidigbi, J.A. Comparative Analysis of Stable Aqueous Dispersion of Silver Nanoparticle Comparative Analysis of Stable Aqueous Dispersion of Silver Nanoparticle Synthesized from Mangifera Indica and Azadirachta Indica Leaf Extract. *Asian Research Association* **2022**, 0–*10*, https://doi.org/10.54392/nnxt2241.
38. Pawar, A.A.; Sahoo, J.; Verma, A.; Alswieleh, A.M.; Lodh, A.; Raut, R.; Lakkakula, J.; Jeon, B.H.; Islam, M.R. Azadirachta Indica -Derived Silver Nanoparticle Synthesis and Its Antimicrobial Applications. *Journal of Nanomaterials* **2022**, *2022*, https://doi.org/10.1155/2022/4251229.
39. Widatalla, H.A.; Yassin, L.F.; Alrasheid, A.A.; Rahman Ahmed, S.A.; Widdatallah, M.O.; Eltilib, S.H.; Mohamed, A.A. Green Synthesis of Silver Nanoparticles Using Green Tea Leaf Extract, Characterization and Evaluation of Antimicrobial Activity. *Nanoscale Advances* **2022**, *4*, 911–915, https://doi.org/10.1039/d1na00509j.
40. Madhavi, J. Comparison of Average Crystallite Size by X - Ray Peak Broadening and Williamson – Hall and Size – Strain Plots for - VO 2 + Doped ZnS / CdS Composite Nanopowder. *SN Applied Sciences* **2019**, *1*, 1–12, https://doi.org/10.1007/s42452-019-1291-9.
41. Asimuddin, M.; Shaik, M.R.; Adil, S.F.; Siddiqui, M.R.H.; Alwarthan, A.; Jamil, K.; Khan, M. Azadirachta Indica Based Biosynthesis of Silver Nanoparticles and Evaluation of Their Antibacterial and Cytotoxic Effects. *Journal of King Saud University - Science* **2020**, *32*, 648–656, https://doi.org/10.1016/j.jksus.2018.09.014.
42. Haroon, M.; Zaidi, A.; Ahmed, B.; Rizvi, A.; Khan, M.S.; Musarrat, J. Effective Inhibition of Phytopathogenic Microbes by Eco-Friendly Leaf Extract Mediated Silver Nanoparticles (AgNPs). *Indian Journal of Microbiology* **2019**, *59*, 273–287, https://doi.org/10.1007/s12088-019-00801-5.
43. Nisar, P.; Ali, N.; Rahman, L.; Ali, M.; Shinwari, Z.K. Antimicrobial Activities of Biologically Synthesized Metal Nanoparticles: An Insight into the Mechanism of Action. *Journal of Biological Inorganic Chemistry* **2019**, *24*, 929–941, https://doi.org/10.1007/s00775-019-01717-7.
44. Mansoor, S.; Zahoor, I.; Baba, T.R.; Padder, S.A.; Bhat, Z.A.; Koul, A.M.; Jiang, L. Fabrication of Silver Nanoparticles Against Fungal Pathogens. *Frontiers in Nanotechnology* **2021**, *3*, 1–12, https://doi.org/10.3389/fnano.2021.679358.
45. Dakal, T.C.; Kumar, A.; Majumdar, R.S.; Yadav, V. Mechanistic Basis of Antimicrobial Actions of Silver Nanoparticles. *Frontiers in Microbiology* **2016**, *7*, 1–17, https://doi.org/10.3389/fmicb.2016.01831.
46. Molina-Hernández, J.B.; Scroccarello, A.; Della Pelle, F.; De Flaviis, R.; Compagnone, D.; Del Carlo, M.; Paparella, A.; Chaves López, C. Synergistic Antifungal Activity of Catechin and Silver Nanoparticles on Aspergillus Niger Isolated from Coffee Seeds. *Lwt* **2022**, *169*, https://doi.org/10.1016/j.lwt.2022.113990.